Biological Psychiatry: CNNI

Archival Report

Cortical Morphometry in the Psychosis Risk Period: A Comprehensive Perspective of Surface Features

Katherine S.F. Damme, Tina Gupta, Robin Nusslock, Jessica A. Bernard, Joseph M. Orr, and Vijay A. Mittal

ABSTRACT

BACKGROUND: Gyrification features reflect brain development in the early prenatal environment. Clarifying the nature of these features in psychosis can help shed light on the role of early developmental insult. However, the literature is currently widely discrepant, which may reflect confounds related to formally psychotic patient populations or overreliance on a single feature of cortical surface morphometry (CSM).

METHODS: This study compares CSM features of gyrification in clinical high-risk (n = 43) youths during the prodromal risk period to typically developing control subjects over two time points across three metrics: local gyrification index, mean curvature index, and sulcal depth (improving resolution and examination of change over 1 year).

RESULTS: Gyrification was stable over time, supporting the idea that gyrification reflects early insult rather than abnormal development or reorganization associated with the disease state. Each of the indices highlighted unique, aberrant features in the clinical high-risk group with respect to control subjects. Specifically, the local gyrification index reflected hypogyrification in the lateral orbitofrontal cortex, superior bank of the superior temporal sulcus, anterior isthmus of the cingulate gyrus, and temporal poles; the mean curvature index indicated sharper gyral and flatter or wider sulcal peaks in the cingulate, postcentral, and lingual gyrus; sulcal depth identified shallow features in the parietal, superior temporal sulcus, and cingulate regions. Further, both the mean curvature index and sulcal depth converged on abnormal features in the parietal cortex.

CONCLUSIONS: Gyrification metrics suggest early developmental insult and provide support for neurodevelopmental hypotheses. Observations of stable CSM features across time provide context for interpreting extant studies and speak to CSM as a promising stable marker and/or endophenotype. Collectively, findings support the importance of considering multiple CSM features.

Keywords: Cortical surface, Curvature index, Gyrification, Morphometry, Prodrome, Psychosis, Schizophrenia, Sulcal depth

https://doi.org/10.1016/j.bpsc.2018.01.003

Cortical surface morphometry (CSM) may provide critical insight into the timing of developmental insults or pathogenic factors that contribute to psychotic disorders (1,2). Indeed, gyrification (a CSM feature parametrized by local gyrification index [lGI], mean curvature index [MCI], and sulcal depth) may reflect abnormal connectivity in utero and in early development, as cortical folding reflects late second– and third-trimester integrity of corticocortical and subcortical connectivity (1,2). Gyrification measured in late adolescence and early adulthood may be relatively unchanged by adolescent neuromaturational processes that drive instability in other cortical features (3). This relative stability suggests that gyrification metrics may provide unique insight into the contribution of early development to risk for psychosis (2,3).

Unfortunately, little is known about the contributions of early brain development to psychosis because clinical markers of psychosis often appear in late adolescence to early adulthood, when neuromaturational processes have already obscured early development (3). Indirect evidence suggests a link between early brain development and increased rates of psychosis from prenatal famine and/or malnutrition (4,5), flu exposure (6,7), and deletions of genes related to early brain development (i.e., 22q11 deletion) (8,9). Furthermore, other established markers of early prenatal development (e.g., dermatoglyphics) relate to psychosis (10,11) but do not provide a direct metric of brain development. Gyrification may provide a more direct metric of early brain development and added insight into abnormal neurodevelopmental processes in psychosis.

 ISSN: 2451-9022

With regard to schizophrenia, the CSM literature is inconsistent (12–14). These inconsistencies may be due in part to variations in methodological approaches and confounds associated with schizophrenia (e.g., substance dependence and medications) (15–17). As a result, it is unknown whether gyrification abnormalities reflect early insult alone and remain unchanged during the prodromal period. Alternatively, gyrification may be subject to later neurodegenerative or putative risk factors such as medication or substance abuse. If stable, gyrification would provide an early marker of prenatal insult that persists across pubertal neuromaturation. Additionally, gyrification metrics may confer additional sensitivity to detecting risk for psychosis, thus adding insight from prenatal development that complements structural metrics of prodromal neural reorganization (e.g., cortical thickness) (18–20).

Evaluating clinical high-risk (CHR) populations (i.e., youths exhibiting prodromal syndromes indicating imminent risk for psychotic disorders prior to psychosis onset) can provide predictive biomarkers as well as insight into pathogenic processes. While this group does exhibit some of the same types of confounds as seen in patients with schizophrenia overall, individuals in this period tend to show fewer factors that convolute results than do populations with chronic psychosis (e.g., medication rates and doses are often lower). With respect to CSM, the few studies that focus on CHR populations do indicate surface abnormalities in these individuals (15–16,21–22). Nevertheless, there is no comprehensive understanding of CSM in CHR individuals, as these investigations rely on a single CSM metric at a single time point (see the Supplement for a review and comparison of metrics). Examining multiple time points of CSM features may establish whether gyrification reflects a preexisting early insult or pathogenic processes during the CHR period. This approach may provide insight into these features in schizophrenia and spectrum populations; specifically, this will help to determine if CSM features are sensitive to neurodegenerative processes or putative environmental factors (see Table 1; see the Supplement for review of relevant literature).

The current study evaluates three metrics of gyrification: /GI, MCI, and sulcal depth. The /GI is the ratio of an outer surface contour to buried cortical surface that employs advanced computation in three dimensions of gyrification rather than relying on a single orientation, such as gyrification index (23,24). While the /GI provides invaluable information, it references an individualized contour; taking this approach in isolation may obscure the exact nature of the specific gyral morphometry. A solution to this issue may lie in incorporating additional measures such as MCI. MCI quantifies each vertex in terms of the radius of osculating circles from the peak of each gyrus (25). This CSM metric provides further sensitivity to changes on a smaller scale and information about the shape of a given arc (i.e., higher MCI implies a sharper curve, while lower numbers represent a wider arc) (26). Finally, sulcal depth provides unique and complementary estimates of linear distance from a reference midpoint surface (i.e., the global midpoint between the gyri and sulci) (27). Thus, incorporating three metrics provides a more comprehensive and nuanced perspective, which includes an inner-to-outer surface ratio, a curve reference, and linear height and/or depth.

By incorporating data across two scan sessions and combining complementary indices (/GI, MCI, and sulcal depth) in a single population, we provide a more comprehensive account of CSM differences (see the Supplement for a review of metrics) in CHR individuals. In addition, this study benefits from incorporating data from two scan sessions, an approach that improves the likelihood of accounting for additional variance and noise (e.g., the variance in gyrification related to scan slice angle in image acquisition) (17,24) and stability of CSM variables. Further, examining CSM features over time allows for a novel perspective that clarifies if CSM features reflect a stable vulnerability trait or something that shifts as a function of pathogenic processes in the CHR period.

In the present investigation, 81 participants (43 CHR and 38 healthy control [HC] participants) completed clinical interviews, a structural scan at a baseline, and then a second scan 12 months later. We evaluated gyrification features from large-scale folding ratios (/GI), shape of the curve (MCI), and the height and/or depth of gyri and sulci (sulcal depth) in both groups (Supplement). We predicted that these CSM features develop in utero and are relatively insensitive to developmental and environmental factors. Past findings suggested both hyper- and hypogyrification in schizophrenia (12,14,28). Similarly, gyrification index, folding index, and /GI studies in CHR youths indicate widespread aberrant

Table 1. Review of Psychosis Literature on Gyrification Cortical Surface Morphometry

Author	*N*	Population	Metric	Findings
Harris *et al.*, 2004 (15)	128	GHR	Gyrification index	Related to conversion
Harris *et al.*, 2007 (30)	34	FEP	Gyrification index	Abnormal at first episode of psychosis
Kulynych *et al.*, 1997 (12)	9	SZ	Gyrification index	Frontal hypergyrification
Sasabayashi *et al.*, 2017 (31)	104	CHR	/GI	Related to conversion
Sasabayashi *et al.*, 2017 (32)	62	FEP	/GI	Abnormal at first episode of psychosis
Bakker *et al.*, 2016 (37)	36	CHR n = 18; 22q11 deletion n = 18	/GI	Related to the 22q11 deletion
Mihailov *et al.*, 2017 (57)	71	22q11 deletion	/GI	Related to the 22q11 deletion
deWit *et al.*, 2017 (54)	24	CHR	/GI	Related to clinical severity at follow-up
Palaniyappan *et al.*, 2011 (14)	57	SZ	/GI	Frontal hypogyrification
Takahashi *et al.*, 2013 (22)	64	FEP	Sulcal depth	Related to deficits in executive function
Csernansky *et al.*, 2008 (42)	33	SZ	Sulcal depth	Asymmetric sulcal depth in temporal lobes

CHR, clinical high-risk; FEP, first-episode psychosis; GHR, genetic high risk; /GI, local gyrification index; SZ, schizophrenia.

gyrification (15–16,21,29–32), with little convergence outside the frontal and temporal regions. From this literature, we predicted that CHR youths would show aberrant /GI in frontal and temporal regions. There is no current guiding literature on curvature, and so we investigated curvature as an exploratory analyses. Based on limited evidence in the olfactory cortex indicating shallow sulcal depth in CHR youths (22), we predicted shallower peaks and depths for sulcal depth. Further, we predicted that there would be no difference in slope between time points, indicating the relative stability of gyrification over time. Finally, we aimed to examine how the features relate to one another; any areas of overlap (where the CHR group shows abnormalities compared with HC group) were evaluated in both a quantitative and qualitative fashion.

METHODS AND MATERIALS

A total of 81 participants (CHR n = 43, HC n = 38) were recruited through the Adolescent Development and Preventive Treatment program. CHR inclusion criteria were based on the presence of a prodromal syndrome (33) and not genetic risk. Demographic and positive symptom characteristics of the sample are described in Table 2 (see the Supplement for exclusion and recruitment criteria). The Structured Interview for Prodromal Syndromes (34) was used to diagnose CHR syndromes. Participants were also given the Word Reading subtest of the fourth edition of the Wide Range Achievement Test as a measure of general intelligence. The Wide Range Achievement Test is a well-validated and broadly used measure of achievement and broad learning ability for adolescents and young adults (35).

A 3T Siemens Tim Trio magnetic resonance imaging scanner (Siemens Corp., Munich, Germany) using a standard 12-channel head coil acquired two scans approximately 1 year apart. Structural images were collected on a T1-weighted three-dimensional magnetization prepared rapid gradient multiecho sequence (sagittal plane; repetition time [TR] 2530 ms; echo times [TE] 51.64 ms, 3.5 ms, 5.36 ms, 7.22 ms, and 9.08 ms; generalized autocalibrating partially parallel acquisitions (GRAPPA) parallel imaging factor of 2; 1-mm^3 isotropic voxels, 192 interleaved slices; field of view 525 mm; flip angle 57°). The Query Design Estimate Contrast tool in the FreeSurfer 6.0 program generated the group contrasts in a general linear model, controlling for gender and medication status, and compared MCI and sulcal depth at each vertex. The /GI was calculated using the general linear model tools (24). (For full data acquisition parameters and preprocessing see the Supplement). The Query Design Estimate Contrast tool in the FreeSurfer program generated the group contrasts in a repeated-measure analysis of variance, controlling for gender and medication status, and compared MCI and sulcal depth at each vertex. To examine gyrification stability, an interclass correlation compared the CSM metrics for each time point for significant clusters to reduce the number of comparisons to the relevant vertices discussed below. These analyses treat FreeSurfer's standardized algorithm as a single, stable rater of CSM metrics in a fixed-rater model of class correlation, which was used in the Psych package of R v.3.1.2 (36). While the Cronbach α is typically reported, the Guttman λ has been reported here, as it better takes into account the variance of the data (36); see the Supplement for a full description.

RESULTS

Group Comparison of the CSM Gyrification Metrics

In whole-brain analyses, the CHR and HC groups differed in gyrification (false discovery rate–corrected $p < .05$ across both hemispheres and Bonferroni corrected for three metric comparisons). The analyses revealed six significant clusters where the /GI differed by group after controlling for gender and antipsychotic status (Figure 1, Table 3). In the left hemisphere, the CHR group showed a decreased /GI, or reduction in the outer surface–to–inner surface ratio, signifying less gyrification, in the bank of the superior temporal sulcus and the temporal pole. In the right hemisphere, the CHR group showed a reduction in /GI, or less gyrification, in the lateral orbitofrontal cortex, bank of the superior temporal sulcus, parahippocampal gyrus, and fusiform gyrus. Interestingly, no cluster demonstrated increased gyrification in the CHR group, suggesting hypogyrification in the CHR group compared with that of the HC group.

Whole-brain analyses revealed nine significant clusters where MCI differed by group (Figure 2, Table 4). For many

Table 2. Demographic Characteristics

	CHR Group	Control Group	Total	Statistic	p
Age, Years, Mean (SD)	18.98 (1.30)	19.13 (1.51)	19.05 (1.40)	$t_{74} = -0.49$	.63
Gender, n					
Male	28	13	40	$\chi^2_1 = 7.71$	.005
Female	15	25	41		
Total	43	38	81		
Education, Years, Mean (SD)	12.67 (1.44)	13.05 (1.83)	12.85 (1.64)	$t_{70} = -1.04$	.30
Parent Education, Years, Mean (SD)	15.66 (2.89)	15.71 (2.60)	15.68 (2.74)	$t_{79} = -0.08$	.94
Symptom Domains, Mean (SD)[a]					
Positive baseline	11.72 (3.50)	0.66 (1.40)	6.53 (6.18)	$t_{1,79} = 18.23$	≤.001
Positive follow-up	10.44 (5.95)	0.32 (0.66)	5.69 (6.68)	$t_{1,79} = 10.44$	≤.001
Wide Range Achievement Test Score, Mean (SD)	108.88 (12.02)	104.40 (11.82)	106.79 (12.09)	$t_{73} = 1.62$	.11

CHR, youths exhibiting prodromal syndromes indicating imminent risk for psychotic disorders prior to psychosis onset.
[a]Positive symptoms reflect total sums from domains from the Structured Interview for Prodromal Syndromes.

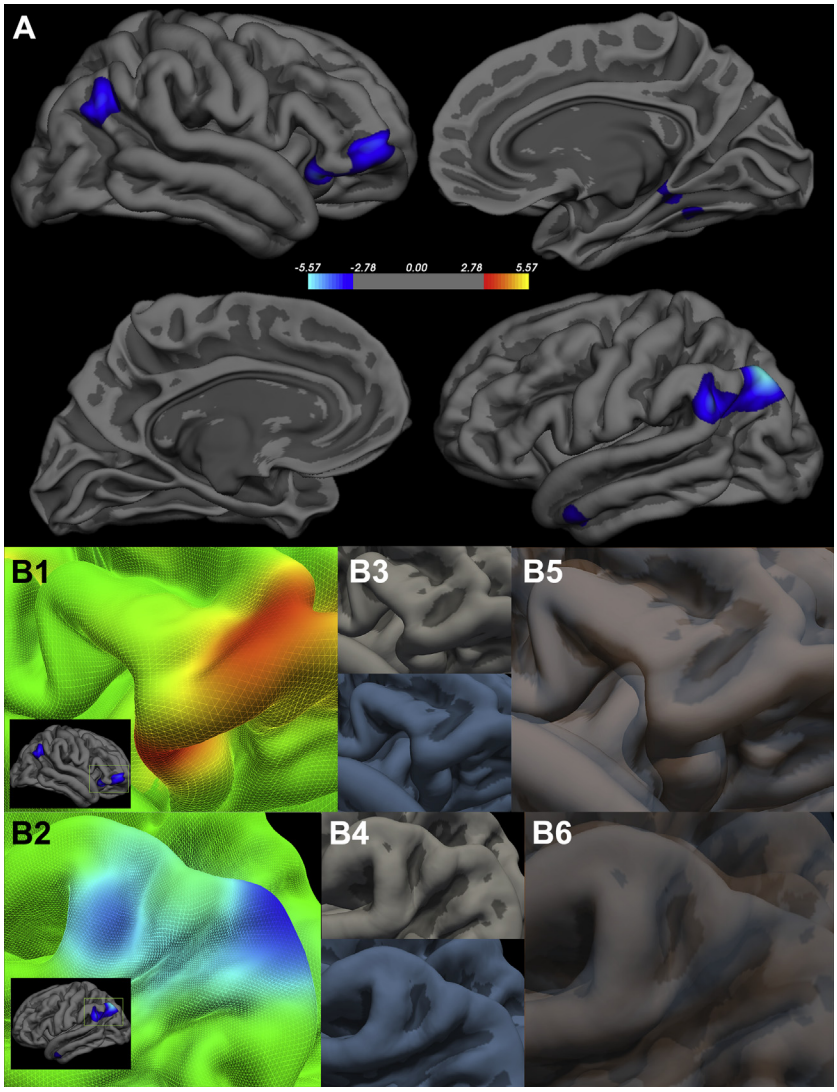

Figure 1. Local gyrification index of clinical high-risk subjects compared with that of healthy control subjects. The images show the right-hemisphere **(A, top)** and left-hemisphere **(A, bottom)** false discovery rate–corrected $p < .05$. Panel **(B)** highlights peak clusters (group statistical images shown in **B1** and **B2**) to demonstrate how each feature varies between the clinical high-risk subjects (group average shown in blue **[B4, bottom]**) and healthy control subjects (group average shown in gray **[B3, top]**). The group average images were overlaid to highlight the surface differences **(B5, B6)**.

regions on the left hemisphere, the CHR group demonstrated a decreased MCI, or sharper gyral curves, in the lingual gyrus, inferior parietal lobule, and postcentral gyrus. A single left-hemisphere cluster demonstrated opposing results, with the fusiform gyrus showing sharper gyrification in the CHR group. In the right hemisphere, the CHR group showed a decreased MCI with decreased peak angles in the superior parietal lobule, isthmus of the cingulate gyrus, and superior parietal lobule. A single right-hemisphere cluster demonstrated opposing results in a sulcus of the superior parietal lobule, which showed sharper gyrification in the CHR group.

In each hemisphere, the CHR and HC groups differed in sulcal depth. The analyses revealed nine significant clusters where sulcal depth differed by group after controlling for gender and antipsychotic status (Figure 3, Table 5). In the left hemisphere, the CHR group showed decreased sulcal depth, or gyral height from the cortical midpoint, in the postcentral gyrus, posterior cingulate, rostral middle frontal gyrus, and lingual gyrus. Again, there was a single cluster of increased sulcal depth on the fusiform gyrus. In the right hemisphere, the CHR group had decreased sulcal depth in gyral areas of the superior parietal lobule and anterior cingulate with a single cluster of increased sulcal depth in the CHR group in the superior parietal lobule.

Comparison of CSM Across Metrics and Time

To evaluate whether CSM clusters converge on vertices or identify unique vertices of surface morphometry, significant clusters were overlaid pairwise, generating two unique masks: a convergence map (containing vertices where metrics overlap on CSM abnormalities) and a uniqueness map (demonstrating the unique information provided by each metric) (Table 5,

Table 3. Talairach Coordinates of Regions Showing Group Differences—Comparing Control Participants With Clinical High-Risk Participants—in Local Gyrification Index

Hemisphere	*p* Value	Size, mm^2	Talairach Coordinates			Region
			x	y	z	
Left	>.00001	3285.18	−34.9	−69.5	45.4	Bank of the superior temporal sulcus
	>.001	351.98	−51.8	−0.2	−28.2	Temporal pole
Right	>.0001	1833.49	42.3	26.5	−14.4	Lateral orbitofrontal cortex
	>.0001	1163.56	49.5	−57.8	32.1	Bank of the superior temporal sulcus
	>.001	720.58	26.3	−42.1	−6.8	Parahippocampal gyrus
	>.001	30.13	47.9	−66.7	14.3	Fusiform gyrus

Figure 4). Spatial convergence of significant voxels occurred between only two metrics, MCI (19.5% of vertices overlap in the left hemisphere; 28.72% of vertices overlap in the right hemisphere) and abnormal sulcal depth (34.61% of vertices overlap in the left hemisphere; 26.44% of vertices overlap in the right hemisphere). Qualitatively, while the ratio metric of *l*GI demonstrated distinct gyrification in frontal and temporal regions, the geometric distance and shape metrics, MCI, and sulcal depth clusters were primarily in parietal, occipital, and cingulate regions, respectively (Supplemental Table S1).

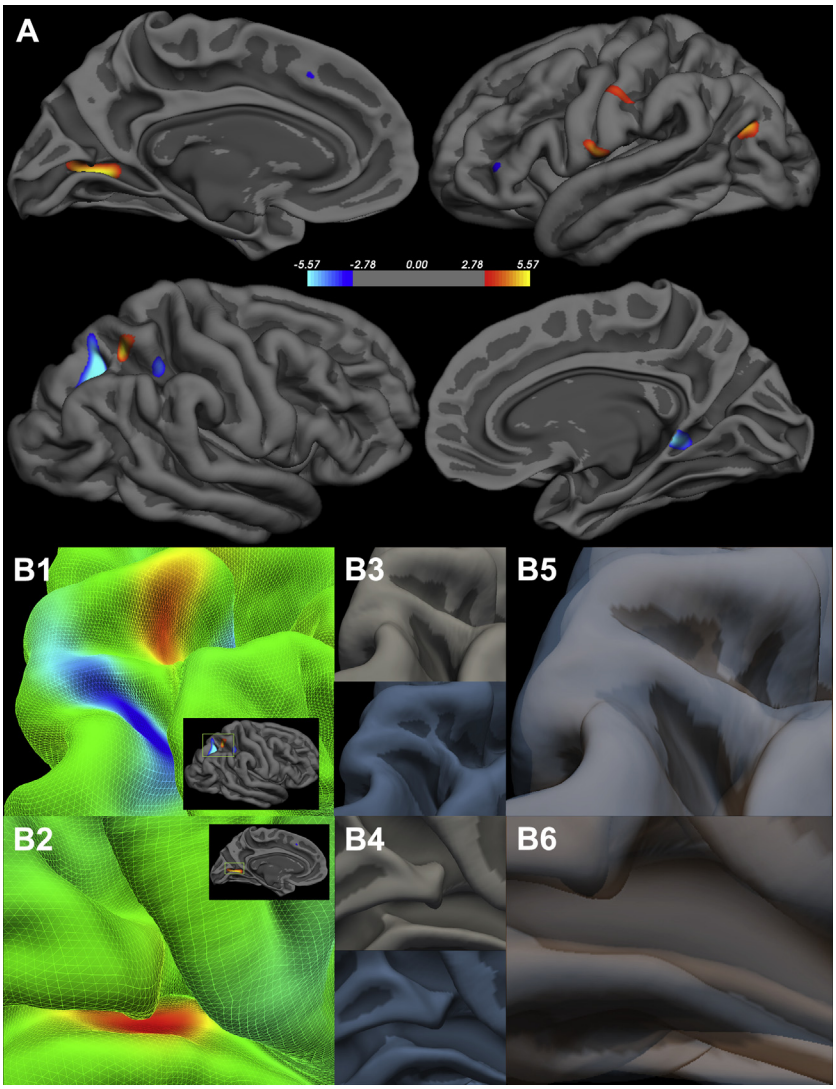

Figure 2. Mean curvature index of clinical high-risk subjects compared with that of healthy control subjects. **(A)** The images show the right-hemisphere (top) and left-hemisphere (bottom) false discovery rate–corrected $p < .05$. Panel **(B)** highlights peak clusters (group statistical images shown in **B1** and **B2**) to demonstrate how each feature varies between the clinical high-risk subjects (group average shown in blue **[B4, bottom]**) and the healthy control subjects (group average shown in gray **[B3, top]**). The group average images were overlaid to highlight the surface differences **(B5, B6)**.

Table 4. Talairach Coordinates of Regions Showing Group Differences—Comparing Control Participants With Clinical High-Risk Participants—in Mean Curvature Index

Hemisphere	*p* Value	Size, mm^2	Talairach Coordinates			Region
			x	y	z	
Left	>.00001	356.18	−21.8	−67.9	0.8	Lingual gyrus
	>.0001	148.75	−36.7	−13.2	−28.3	Fusiform gyrus
	>.0001	136.46	−40.2	−71.3	20.5	Inferior parietal lobule
	>.0001	69.97	−60.3	−7	11.8	Postcentral gyrus
	>.001	50.01	−57	−17.6	37.4	Postcentral gyrus
Right	>.000001	318.16	21.7	−65.5	37.5	Superior parietal lobule
	>.0001	182.77	26.7	−54.2	53.8	Superior parietal lobule
	>.0001	116.57	13.5	−42.3	−0.3	Isthmus of the cingulate gyrus
	>.0001	67.43	32.4	−44	44.5	Superior parietal lobule

To use both time points as a converging data point, we tested the assumption that the gyrification is stable over time. These time points also provided us with a unique opportunity to confirm the stability of gyrification and assess whether these metrics changed during the prodromal period. Across all participants, the CSM metrics were significantly and highly stable over time (Supplement). These measures were also highly reliable: *I*GI (λ = .92), MCI (λ = .86), and sulcal depth (λ = .93). In parallel analyses, the CHR group did not significantly vary in the stability of their CSM (Supplemental Table S2). Follow-up analyses compared peak clusters with symptoms (Supplement and Supplemental Table S3).

DISCUSSION

This study was highly innovative in examining a number of CSM characteristics over two time points (1 year apart) during the CHR period. This approach yielded several important findings. First, CSM characteristics appeared highly stable over time, which has relevance for informing conceptual models of psychosis. Next, we observed distinct abnormalities in CSM features across cingulate, parietal, orbitofrontal, and superior temporal regions. Further, we detected clusters of aberrant CSM matrices that converged on the parietal lobule. Taken together, this novel approach was effective in providing a comprehensive perspective that yielded new discoveries about CSM features. Specifically, each index highlighted unique aberrant features in the CHR group, which would have been missed if we had employed a single-variable approach. With *I*GI, CHR participants exhibited hypogyrification in the lateral orbitofrontal cortex, superior bank of the superior temporal sulcus, anterior isthmus of the cingulate, and temporal poles. For curvature, the CHR youths had both sharper peaks on the gyri and flatter and/or wider sulcal peaks in the posterior isthmus of the cingulate, postcentral gyrus, and lingual gyrus. For sulcal depth, we observed shallower overall gyrification in the CHR youths, with distinct local parietal, parietal operculum, inferior bank of the superior temporal sulcus, and rostral cingulate regions.

In line with predictions, there was abnormal gyrification in the CHR group in the temporal and frontal lobes. The evaluation of *I*GI identified entirely spatially unique clusters where groups differed. The distinct spatial and conceptual information (i.e., local ratios rather than linear or arc metric) provided by this metric highlights the importance integrating multiple metrics of CSM features. The CHR group demonstrated hypogyrification compared with the HC group, and this finding is consistent with reports from other studies of CHR participants. Bakker *et al.* (37) found a similar hypogyrification pattern that was predictive of later symptoms. Similarly, Hirjak *et al.* (38) found clinical features related to aberrant gyrification along the bank of the superior temporal sulcus, a region that was also identified in the current study. Finally, these findings are consistent with single–time-point analyses of CHR (31,32), first-episode psychosis (31,32), and schizophrenia (39), in which investigators found similar patterns of gyrification in the temporal, frontal, and parahippocampal regions when compared with those of control subjects.

Group comparisons of MCI, an understudied metric of gyrification, revealed distinct parietal geometry of gyrification related to the CHR group. This metric indicated many clusters in the parietal lobe, demonstrating steeper, sharper curves on the edge of gyri and wider curves within the sulci. While no previous studies of CHR individuals have investigated MCI, studies of schizophrenia do demonstrate a pattern of parietal sulcal curvature distinct from that of control subjects (40). Drawing instead from related work in connectivity (41) and other metrics of gyrification (31–32,39), investigators have found ample evidence relating superior temporal, orbitofrontal, cingulate, and parietal regions in psychosis in adolescence, but none of these findings have been taken directly from MCI. Here, we provided further support for the notion that MCI may be a useful metric of pathological early development, identifying distinct CHR cingulate curvature features not previously identified in the literature. Importantly, MCI was sensitive to the CSM features that would not have been identified by examining *I*GI alone. While several MCI features converged with sulcal depth to identify surface features that distinguished CHR from HC groups, 76.4% of voxels identified by MCI were unique. This MCI-specific pattern highlighted again the importance of a comprehensive approach to analyzing CSM features. Furthermore, while common CSM-feature sites were identified, each metric provided unique conceptual information about these voxel sites. Specifically, MCI identified distinct shape features of curvature but provided no insight into the gray matter to white matter ratio or height or depth of gyri and sulci.

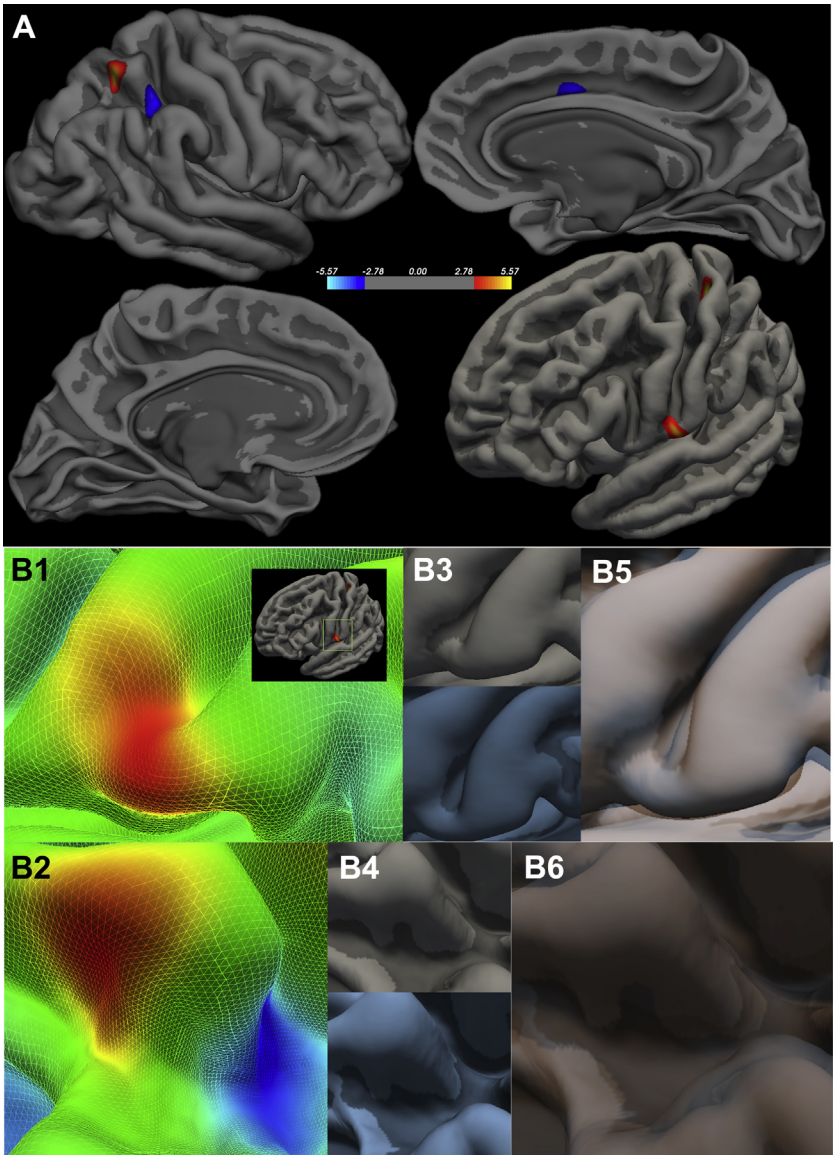

Figure 3. Sulcal depth of clinical high-risk subjects compared with that of healthy control subjects. The images show the right-hemisphere **(A, top)** and **(A, bottom)** left-hemisphere false discovery rate–corrected $p < .05$. Panel **(B)** highlights peak clusters (group statistical images shown in **B1** and **B2**) to demonstrate how each feature varies between the clinical high-risk subjects (group average shown in blue **[B4, bottom]**) and healthy control subjects (group average in shown in gray **[B3, top]**). The group average images were overlaid to highlight the surface differences **(B5, B6)**.

The sulcal depth group analysis indicated aberrant structure in the CHR group, largely in parietal, opercular, and cingulate regions. While the only CHR study of sulcal depth focused on a region of interest in the olfactory sulcus (22), the current parietal pattern of sulcal-depth abnormalities is consistent with findings that identified postcentral and parietal opercular regions of aberrant sulcal depth in schizophrenia (42). While many CSM features overlapped with the features identified by MCI, several of the clusters of sulcal-depth metrics were distinct in their identification of critical clusters. Additionally, sulcal depth provided unique information about these clusters. MCI indicated that parietal clusters fall away more steeply into wider sulcal curves, and sulcal-depth findings suggested that these curves were also shallower in sulcal depth. Taken together, the HC group had both higher gyri and lower sulci compared with those of the CHR group in these clusters.

The neural diathesis-stress conceptualization of psychosis suggests that genetic factors and early developmental insults confer early vulnerability for psychosis. Then later, in adolescence, this preexisting aberrant CSM-feature vulnerability interacts with neuromaturational factors. This interaction of early and neuromaturational factors—both normative and pathological brain development—eventually forms psychotic symptoms (20,43,44). Examining the adolescent period immediately preceding onset yielded many important findings. However, our understanding of both the early insult period and how early insult later interacts with pubertal factors is limited.

The present findings provide two important advancements in this regard. First, youths who met criteria for a prodromal syndrome did, in fact, show marked brain characteristics that may speak to an early insult, as CSM features developed and hardened in response to connectivity. Second, the present results provide a new perspective on the stability of CSM

Table 5. Talairach Coordinates of Regions Showing Group Differences—Comparing Control Participants With Clinical High-Risk Participants—in Sulcal Depth

Hemisphere	*p* Value	Size, mm^2	Talairach Coordinates			Region
			x	y	z	
Left	>.00001	259.45	−35.3	−30.8	58.3	Postcentral gyrus
	>.0001	137.32	−59.9	−6.7	11.7	Postcentral gyrus
	>.0001	32.54	−10.7	−28.3	38.5	Posterior cingulate gyrus
	>.0001	20.1	−36.4	−13.4	−29.1	Fusiform gyrus
	>.001	13.85	−44.2	32.4	23.2	Rostral middle frontal
	>.001	15.89	−7.2	−72.2	4	Lingual gyrus
Right	>.00001	238.92	28.4	−54.1	58.2	Superior parietal lobule
	>.0001	212.01	31.7	−43.4	45.2	Superior parietal lobule
	>.001	94.53	11	13.5	34.5	Caudal anterior cingulate gyrus

features across adolescent neuromaturational processes in both CHR individuals and control subjects. While gyrification developed in tandem with brain connectivity in utero (45), most studies emphasized neural development in the adolescent prodromal period (29,46). The vast adolescent neuromaturational changes led researchers to question whether CSM features undergo further changes in the prodrome or after onset (15,16). Additionally, present findings suggest that gyrification was remarkably static, which has implications for the way we view stable versus changing vulnerability factors in a period of active normative and pathological development. Additionally, these findings may affect the way we interpret findings in the context of leading neurodevelopmental (20,44) and disconnectivity conceptualizations of psychosis (18). Finally, *I*GI is a potential early biomarker of risk, distinguishing CHR, psychosis converters, and first-episode psychosis subjects from HC subjects (15,16,30–32). In this regard, CSM gyrification metrics may have added value when combined with gray matter and white matter changes over adolescence in identifying risk and predicting conversion with techniques like machine-learning classification. Additionally, connectomics across metrics of gyrification may refine prediction and individualization of treatment (39).

Altogether, it is particularly interesting that areas that develop earlier (i.e., visual and parietal regions) showed aberrant curvature and sulcal depth, while *I*GI clusters tended toward later developing regions (i.e., frontal lobe and temporal areas). This distinction may be driven by the content of the metrics, as both sulcal depth and MCI exclusively measure gray matter surface features, while *I*GI is also sensitive to the white matter surface features. Therefore, it is possible that our findings in the parietal lobule are reflective of abnormal brain development and connectivity in utero, while the broader regions implicated by *I*GI may also be picking up on aberrant white matter surface features that occurred later in development (myelination). However, it will be important for future larger longitudinal studies with more developmental time points to confirm this possibility. Further, it will be important for future studies to consider how these features contribute uniquely to behavioral and cognitive aspects of psychosis. Additionally, future research should examine whether measures of the prenatal environment such as substance use,

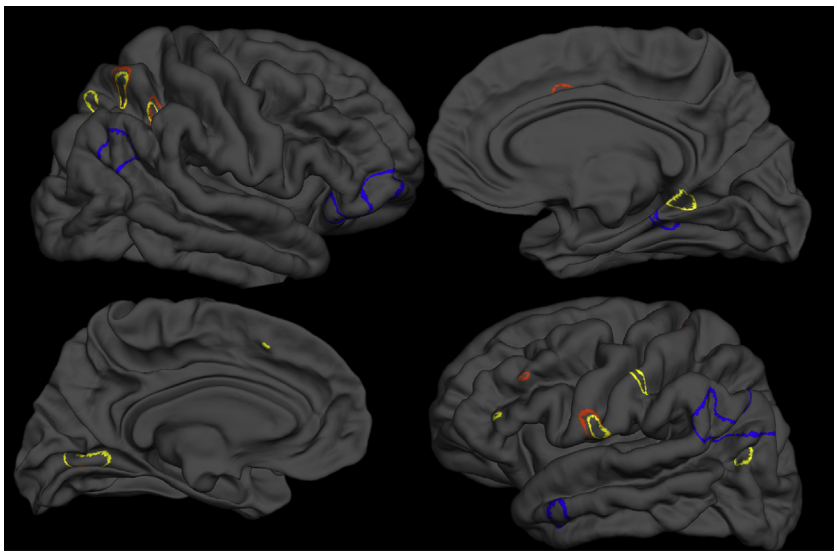

Figure 4. Regional clusters with overlap of significance for local gyrification index (blue), mean curvature index (yellow), and sulcal depth (red).

measures of stress, parental education, parental socioeconomic status, urbanicity (47), obstetric complications, or neurological soft signs such as motor impairment may relate to CSM features (48). It is also important to examine the relationship between gyrification and potentially related metrics such as connectivity and cortical gray matter and white matter volumetrics. Collectively, the findings, indicating substantive novel contributions from each index, support a recommendation that all future studies of CSM features include multiple indices. Furthermore, it will be necessary to investigate conversion longitudinally in separate investigations, as this could be an informative empirical question to apply to psychosis and cortical morphology broadly.

This study shows great promise, but there are still important limitations to consider. While this study sample is comparable to, or larger than, those of other longitudinal studies (17–37 individuals) (15,16,30,49–52), future work could benefit from increased sample sizes. Notably, this represents one of the largest studies in a CHR population to include two scan time points (15,16,30). Additionally, moving forward, it will be important to understand the relationship between CSM features and antipsychotic medication use. While some CSM features (e.g., gray matter volume) are sensitive to antipsychotic medication (53–58), it remains unclear whether gyrification is stable across treatment. This study included only a small number of the CHR participants treated with antipsychotic medications (n = 8) and did not find a significant effect of medication. Nonetheless, the influence of neuroleptic treatment on cortical and subcortical structure remains an important empirical question, and future work, with better-powered studies, should continue to evaluate medication effects on CSM features. Further, this study included an uneven sex distribution between groups (in part reflecting the nature of psychosis), and while we did not detect any effects for sex, future work should carefully evaluate possible sex differences.

ACKNOWLEDGMENTS AND DISCLOSURES

This work was supported by the National Institute of Mental Health (Grant No. 2T32MH067564 to KSFD), and the project was supported by the National Institutes of Health (Grant Nos. RO1MH094650, 1R01MH112545–01, R21/R33MH103231, and R21MH110374 to VAM).

VAM is a consultant to Takeda Pharmaceuticals. The other authors report no biomedical financial interests or potential conflicts of interest.

ARTICLE INFORMATION

From the Department of Psychology (KSFD, TG, RN, VAM), Northwestern University, Evanston, Illinois, and the Department of Psychological and Brain Sciences (JAB, JMO) and Texas A&M Institute for Neuroscience (JAB, JMO), Texas A&M University, College Station, Texas.

Address correspondence to Katherine S.F. Damme, M.S., Department of Psychology, Northwestern University, 2029 Sheridan Road, Evanston, IL 60208; E-mail: Kate.Damme@u.northwestern.edu.

Received Dec 11, 2017; revised Jan 7, 2018; accepted Jan 8, 2018.

Supplementary material cited in this article is available online at https://doi.org/10.1016/j.bpsc.2018.01.003.

REFERENCES

1. Van Essen DC (1997): A tension-based theory of morphogenesis and compact wiring in the central nervous system. Nature 385:313–318.
2. White T, Hilgetag CC (2011): Gyrification and neural connectivity in schizophrenia. Dev Psychopathol 23:339–352.
3. Li G, Wang L, Shi F, Lyall AE, Lin W, Gilmore JH, Shen D (2014): Mapping longitudinal development of local cortical gyrification in infants from birth to 2 years of age. J Neurosci 34:4228–4238.
4. Brown AS, Susser ES (2008): Prenatal nutritional deficiency and risk of adult schizophrenia. Schizophr Bull 34:1054–1063.
5. Mackay E, Dalman C, Karlsson H, Gardner RM (2017): Association of gestational weight gain and maternal body mass index in early pregnancy with risk for nonaffective psychosis in offspring. JAMA Psychiatry 70:339–349.
6. Mednick SA, Machon RA, Huttunen MO, Bonett D (1988): Adult schizophrenia following prenatal exposure to an influenza epidemic. Arch Gen Psychiatry 4:189–192.
7. Brown A (2006): Prenatal infection as a risk factor for schizophrenia. Schizophr Bull 32:200–202.
8. Simon TJ, Ding J, Bish JP, McDonald-McGinn DM, Zackai EH, Gee J (2005): Volumetric, connective, and morphologic changes in the brains of children with chromosome 22q11.2 deletion syndrome: An integrative study. Neuroimage 25:169–180.
9. Gur RE, Bassett AS, McDonald-McGinn DM, Bearden CE, Chow E, Emanuel BS, Owen M, *et al.* (2017): A neurogenetic model for the study of schizophrenia spectrum disorders: The international 22q11.2 deletion syndrome brain behavior consortium. Mol Psychiatry 22:1664–1672.
10. Mittal VA, Dean DJ, Pelletier A (2012): Dermatoglyphic asymmetries and fronto-striatal dysfunction in young-adults reporting non-clinical psychosis. Acta Psychiatr Scand 126:290–297.
11. Russak ODF, Ives L, Mittal VA, Dean DJ (2016): Fluctuating dermatoglyphic asymmetries in youth at ultrahigh-risk for psychotic disorders. Schizophr Res 170:301–303.
12. Kulynych JJ, Luevano LF, Jones DW, Weinberger DR (1997): Cortical abnormality in schizophrenia: an in vitro application of the gyrification index. Biol Psychiatry 41:995–999.
13. Palaniyappan L, Liddle PF (2012): Differential effects of surface area, gyrification and cortical thickness on voxel based morphometric deficits in schizophrenia. Neuroimage 60:693–699.
14. Palaniyappan L, Mallikarjun P, Joseph V, White TP, Liddle PF (2011): Folding of the prefrontal cortex in schizophrenia: regional differences in gyrification. Biol Psychiatry 69:974–979.
15. Harris JM, Whalley H, Yates S, Miller P, Johnstone EC, Lawrie SM (2004): Abnormal cortical folding in high-risk individuals: A predictor of the development of schizophrenia? Biol Psychiatry 56:182–189.
16. Harris JM, Yates S, Miller P, Best JJK, Johnstone EC, Lawrie SM (2004): Gyrification in first-episode schizophrenia: A morphometric study. Biol Psychiatry 55:141–147.
17. Narr KL, Toga AW, Szeszko P, Thompson PM, Woods RP, Robinson D, *et al.* (2005): Cortical thinning in cingulate and occipital cortices in first episode schizophrenia. Biol Psychiatry 58:32–40.
18. Friston K, Brown HR, Siemerkus J, Stephan KE (2016): The dysconnection hypothesis (2016). Schizophr Res 176:83–94.
19. Friston KJ, Frith CD (1995): Schizophrenia: A disconnection syndrome? Clin Neurosci 3:89–97.
20. Walker E, Mittal V, Tessner K (2008): Stress and the hypothalamic pituitary adrenal axis in the developmental course of schizophrenia. Annu Rev Clin Psychol 4:189–216.
21. Jung WH, Kim JS, Jang JH, Choi JS, Jung MH, Park JY, Kwon JS (2011): Cortical thickness reduction in individuals at ultra-high-risk for psychosis. Schizophr Bull 37:839–849.
22. Takahashi T, Nakamura Y, Nakamura K, Ikeda E, Furuichi A, Kido M, *et al.* (2013): Altered depth of the olfactory sulcus in first-episode schizophrenia. Prog Neuropsychopharmacol Biol Psychiatry 40: 167–172.
23. Zilles K, Armstrong E, Schleicher A, Kretschmann H (1988): The human pattern of gyrification in the cerebral cortex. Anat Embryol (Berl) 179:173–179.
24. Schaer M, Cuadra MB, Schmansky N, Fischl B, Thiran JP, Eliez S (2012): How to measure cortical folding from MR images: a step-by-step tutorial to compute local gyrification index. J Vis Exp e3417.

25. Pienaar R, Fischl B, Caviness V, Makris N, Grant PE (2008): A methodology for analyzing curvature in the developing brain from preterm to adult. Int J Imaging Syst Technol 18:42–68.
26. Luders E, Thompson PM, Narr KL, Toga AW, Jancke L, Gaser C (2006): A curvature-based approach to estimate local gyrification on the cortical surface. Neuroimage 29:1224–1230.
27. Fischl B (2012): FreeSurfer. Neuroimage 62:774–781.
28. Wiegand LC, Warfield SK, Levitt JJ, Hirayasu Y, Salisbury DF, Heckers S, *et al.* (2005): An in vivo MRI study of prefrontal cortical complexity in first-episode psychosis. Am J Psychiatry 162:65–70.
29. Cannon TD, Chung Y, He G, Sun D, Jacobson A, Van Erp TG, *et al.* (2015): Progressive reduction in cortical thickness as psychosis develops: A multisite longitudinal neuroimaging study of youth at elevated clinical risk. Biol Psychiatry 77:147–157.
30. Harris JM, Moorhead TWJ, Miller P, McIntosh AM, Bonnici HM, Owens DGC, Lawrie SM (2007): Increased prefrontal gyrification in a large high-risk cohort characterizes those who develop schizophrenia and reflects abnormal prefrontal development. Biol Psychiatry 62: 722–729.
31. Sasabayashi D, Takayanagi Y, Takahashi T, Koike S, Yamasue H, Katagiri N, *et al.* (2017): Increased occipital gyrification and development of psychotic disorders in individuals with an at-risk mental state: A multicenter study. Biol Psychiatry 82:737–745.
32. Sasabayashi D, Takayangagi Y, Nishiyama S, Takahashi T, Furuichi A, Kido M, *et al.* (2017): Increased frontal gyrification negatively correlates with executive function in patients with first-episode schizophrenia. Cereb Cortex 27:2686–2694.
33. Miller TJ, McGlashan TH, Rosen JL, Cadenhead K, Ventura J, McFarlane W, Woods SW (2003): Prodromal assessment with the structured interview for prodromal syndromes and the scale of prodromal symptoms: predictive validity, interrater reliability, and training to reliability [published correction appears in Schizophr Bull 2004;30: following 217]. Schizophr Bull 29:703–715.
34. Miller TJ, McGlashan TH, Woods SW, Stein K, Driesen N, Corcoran CM, *et al.* (1999): Symptom assessment in schizophrenic prodromal states. Psychiatric Q 70:273–287.
35. Wilkinson GS, Robertson GJ (2006): Wide Range Achievement Test, 4th ed. (WRAT4). Lutz, FL: Psychological Assessment Resources.
36. Revelle W. Package 'psych.' Version 1.7.8. Available at: http://personality-project.org/r/psych-manual.pdf. Accessed June 22, 2017.
37. Bakker G, Caan MWA, Vingerhoets WAM, Da Silva-Alves F, De Koning M, Boot E, *et al.* (2016): Cortical morphology differences in subjects at increased vulnerability for developing a psychotic disorder: A comparison between subjects with ultra-high risk and 22q11.2 deletion syndrome. PLoS One 11:1–16.
38. Hirjak D, Kubera KM, Wolf RC, Thomann AK, Hell SK, Seidl U, Thomann PA (2015): Local brain gyrification as a marker of neurological soft signs in schizophrenia. Behav Brain Res 292: 19–25.
39. Palaniyappan L, Marques TR, Taylor H, Mondelli V, Reinders AAT, Bonaccorso S, *et al.* (2016): Globally efficient brain organization and treatment response in psychosis: A connectomic study of gyrification. Schizophr Bull 42:1446–1456.
40. White T, Andreasen NC, Nopoulos P, Magnotta V (2003): Gyrification abnormalities in childhood- and adolescent-onset schizophrenia. Biol Psychiatry 15:418–426.
41. Cho KIK, Shenton ME, Kubicki M, Jung WH, Lee TY, Yun JY, *et al.* (2016): Altered thalamo-cortical white matter connectivity: Probabilistic tractography study in clinical-high risk for psychosis and first-episode psychosis. Schizophr Bull 42:723–731.
42. Csernansky JG, Gillespie SK, Dierker DL, Anticevic A, Wang L, *et al.* (2008): Symmetric abnormalities in sulcal patterning in schizophrenia. Neuroimage 43:440–446.
43. Karlsgodt KH, Sun D, Cannon TD (2010): Structural and functional brain abnormalities in schizophrenia. Curr Dir Psychol Sci 19:226–231.
44. Pruessner M, Cullen AE, Aas M, Walker EF (2017): The neural diathesis-stress model of schizophrenia revisited: an update on recent findings considering illness stage and neurobiological and methodological complexities. Neurosci Biobehav Rev 73:191–218.
45. Collin G, van den Heuvel MP (2013): The ontogeny of the human connectome. Neuroscientist 19:616–628.
46. Mittal VA, Gupta T, Orr JM, Pelletier AL, Dean DJ, Lunsford-Avery JR, Millman ZB (2013): Physical activity level and medial temporal health in youth at ultra high-risk for psychosis. J Abnorm Psychol 122: 1101–1110.
47. Mendez MA, Popkin BM (2004): Globalization, urbanization, and nutritional change in the developing world. In: Globalization of Food Aystems in Developing Countries: Impact on Food Security and Nutrition. Rome, Italy: Food and Agriculture Organisation of the United Nations (FAO), 55–80.
48. Filatova S, Koivumaa-Honkanen H, Hirvonen N, Freeman A, Ivandic I, Hurtig T, *et al.* (2017): Early motor developmental milestones and schizophrenia: A systematic review and meta-analysis. Schizophr Res 188:13–20.
49. Bloemen OJN, de Koning MB, Schmitz N, Nieman DH, Becker HE, de Haan L, *et al.* (2010): White-matter markers for psychosis in a prospective ultra-high-risk cohort. Psychol Med 40:1297–1304.
50. Peters BD, Blaas J, de Haan L (2010): Diffusion tensor imaging in the early phase of schizophrenia: what have we learned? J Psychiatr Res 44:993–1004.
51. von Hohenberg CC, Pasternak O, Kubicki M, Ballinger T, Vu MA, Swisher T, Shenton ME (2014): White matter microstructure in individuals at clinical high risk of psychosis: A whole-brain diffusion tensor imaging study. Schizophr Bull 40:895–903.
52. Walterfang M, McGuire PK, Yung AR, Phillips LJ, Velakoulis D, Wood SJ, *et al.* (2008): White matter volume changes in people who develop psychosis. Br J Psychiatry 193:210–215.
53. Abramovic L, Boks MP, Vreeker A, Bouter DC, Kruiper C, Verkooijen S, *et al.* (2016): The association of antipsychotic medication and lithium with brain measures in patients with bipolar disorder. Eur Neuropsychopharmacol 26:1741–1751.
54. Jørgensen KN, Nesvåg R, Gunleiksrud S, Raballo A, Jönsson EG, Agartz I (2016): First- and second-generation antipsychotic drug treatment and subcortical brain morphology in schizophrenia. Eur Arch Psychiatry Clin Neurosci 266:451–460.
55. deWit S, Ziermans TB, Nieuwenhuis M, Schothorst PF, van Engeland H, Kahn RS, *et al.* (2017): Individual prediction of long-term outcome in adolescents at ultra-high risk for psychosis: Applying machine learning techniques to brain imaging data. Hum Brain Mapp 38:704–714.
56. Insel TR (2010): Rethinking schizophrenia. Nature 468:187–193.
57. Mihailov A, Padula MC, Scariati E, Schaer M, Eliez S (2017): Morphological brain changes associated with negative symptoms in patients with 22q11.2 deletion syndrome. Schizophr Res 188:52–58.
58. Pantelis C, Yücel M, Wood SJ, Velakoulis D, Sun D, Berger G, McGorry PD (2005): Structural brain imaging evidence for multiple pathological processes at different stages of brain development in schizophrenia. Schizophr Bull 31:672–696.